Repeat Subglacial Lake Drainage and Filling beneath Thwaites Glacier

Repeat Subglacial Lake Drainage and Filling beneath Thwaites Glacier

G. Malczyk[1], N. Gourmelen[1], D. Goldberg[1], J. Wuite[2], and T. Nagler[2]

[1]School of Geosciences, University of Edinburgh, Edinburgh, UK.

[2]ENVEO IT GmbH, Innsbruck, Austria.

Corresponding author: George Malczyk (G.R.Malczyk@sms.ed.ac.uk)

Key Points:

- Evidence of a drainage event at the lake region of the Thwaites glacier during 2017, four years after previous activity.
- Contrasting lake behaviors, drainage volume, discharge, and timing of events between the 2013 and 2017 events.
- Observations of recharge rates suggest that modelled melt water production is underestimated.

Abstract

Active subglacial lakes have been identified throughout Antarctica, offering a window into subglacial environments and their impact on ice sheet mass balance. Here we use high-resolution altimetry measurements from 2010 to 2019 to show that a lake system under the Thwaites glacier undertook a large episode of activity in 2017, only four years after the system underwent a substantial drainage event. Our observations suggest significant modifications of the drainage system between the two events, with 2017 experiencing greater upstream discharge, faster lake-to-lake connectivity, and the transfer of water within a closed system. Measured rates of lake recharge during the inter-drainage period are 137% larger than modelled estimates, suggesting processes that drive subglacial meltwater production, such as geothermal heat flux or basal friction, are currently underestimated.

Plain Language Summary

Antarctic subglacial lakes can play an important role in ice sheet dynamics. When subglacial lakes drain, they release large amounts of water that interact with the subglacial drainage system. Here we show lakes draining only four years after a previous drainage event. Our results suggest that lake activity increases the efficiency of the subglacial drainage network. Rates of lake recharge indicate that basal melt-water production is significantly higher than previously thought.

1. Introduction

The vast majority of ice in the Antarctic ice sheet drains from the continent to the ocean through fast-flowing ice streams and glaciers (Rignot et al., 2011). The presence of meltwater at the bed reduces basal stress, allowing the ice masses to sustain high velocities in some regions (Alley et al., 1986; Kamb, 2001). The movement of water has also been linked to transient glacier flow acceleration (Stearns et al., 2008) and to enhanced melt at the grounding line (Le Brocq et al., 2013; Wei et al., 2020). Therefore, the presence, location, and movement of water at the ice-bed interface are likely significant controls on the mass balance of Antarctica (Bell, 2008). The transport of water from upstream regions to downstream zones was once thought to be a steady-state process (Parizek et al., 2002); however, satellite observations indicate that the movement of subglacial water might be episodic (Gray *et al.,* 2005; Wingham *et al.*, 2006). Observations of localized height anomalies have been interpreted as subglacial water moving in and out of subglacial lakes causing a response at the surface of the glacier. Subglacial lakes located within the interior of the ice sheet are thought to be in a steady state with only localized impact on ice flow (Siegert et al., 2005), whilst lakes located in fast-flowing regions could temporarily alter Antarctic mass balance by modulating the amount and location of subglacial water through episodic drainage events (Siegfried et al., 2018).

Active subglacial lakes have been identified throughout Antarctica with satellite altimetry and ice-penetrating radar (Smith et al., 2009; Wright and Siegert, 2012). Observations of surface elevation changes indicate that subglacial lakes are hydraulically connected (Fricker & Scambos, 2009; Wingham et al., 2006), and often exist in groups beneath Antarctic ice streams. During the ICESat-1 mission, operating from 2003 to 2010, no subglacial lakes were observed under the Amundsen Sea Sector of the Antarctic Ice Sheet, which was attributed to inadequate measurements due to cloudy conditions (Smith et al., 2017). Analysis of ice-penetrating radar

identified a region of high specularity under the Thwaites glacier, interpreted as evidence of the presence of water in distributed channels at the base of the ice sheet (Schroeder et al., 2013). In 2017, four large connected active subglacial lakes were discovered under the Thwaites Glacier from analysis of swath processed CryoSat-2 data, which indicated that the lakes drained simultaneously between June 2013 and January 2014 (Smith et al., 2017). Examination of the modelled subglacial melt production in the region suggested that the lakes should have a refill and drainage recurrence interval between 5 and 83 years, depending on whether the recharge scenario involved local melt production only, or melt generated across the larger upstream catchments.

Here we use CryoSat-2 altimetry to produce elevation time series which extends the record of lake activity to mid-2019 and describes a second drainage event in 2017. The occurrence of two drainage events within a short timeframe allow us to explore the impact of drainage activity on the evolution of the subglacial system, and to quantify sub-glacial melt supply providing rare insights into sub-glacial processes and basal melt generation.

2. Data and Methods

2.1 Surface elevation and volume change estimates

Time-dependent elevations were generated using swath processing of CryoSat-2 level L1b SARin data acquired between 2010 and 2019. In contrast to the commonly used point of closest approach (POCA), swath processed SARin exploits the full radar waveform to resolve substantially more elevation than that of the POCA (Gourmelen et al., 2018; Gray et al., 2013; Hawley et al., 2009).

To determine the spatial behavior of subglacial lake activity, average rates of surface elevation change were computed using a plane-fitting algorithm (McMillan et al., 2014) applied to swath processed SARin data from late-2014 to mid-2019. Due to the dense elevation field provided by swath processing our region was gridded at a 500-meter posting, with each cell incorporating a search radius of 1.5 km to lower map noise. Within each pixel time-dependent elevations were obtained by fitting a weighted hyperplane against easting, northing, and time; with a time-dependent coefficient retrieved from the regression representing the linear rate of surface change (Foresta et al., 2016). The model was fitted iteratively to the data, omitting elevations differing more than three standard deviations away from the model fit until no further outliers were detected. These maps were used to create masks encapsulating lake activity, which we define as a region with significant localized elevation change (> 0.5 m yr^{-1}) relative to the background signal (Fricker *et al.*, 2007; Flament, Berthier and Rémy, 2014; Smith *et al.*, 2017).

The temporal behavior of the lake system was determined through the creation of a surface elevation change timeseries between 2010 and 2019. We used an adapted version of the point-to-point method (see Text S1 for a detailed description) outlined in *Gray et al.,* (2015) and Gray *et al.,* (2019) over our lake outlines to determine time-dependent elevations at a 45-day resolution, with elevations averaged over a 45-day search radius. To isolate the behavior of each lake relative to the catchment we removed the background thinning signal. This was achieved by

deducing time-dependent elevations, as per the method above, using a 5 km exclusion area around each lake and subtracting it from the lake's signal.

Note that, although the input dataset is similar, both the spatial and temporal approach followed here should lead to slightly different spatio-temporal smoothing compared against previous estimates of 2013 activity. (Smith et al., 2017; see Text S2).

Volume change through time was derived by integrating elevation change against the area of each lake mask. For any time-dependent volume change, an approximate statistical error is given by the average of the standard deviations divided by the square root of the number of timeseries realizations. Our volume estimates typically have a standard error of ± 0.02 km^3. This is a lower bound on our uncertainty, as the method of spatial and temporal sampling are likely to introduce additional uncertainty. In the absence of an alternative approach, we approximate the volume budget of subglacial water flux by the volume corresponding to the surface deflation, although we acknowledge that this assumption leads to additional uncertainty (Smith et al., 2017, Sergienko et al., 2007). Recharge rates were calculated by applying linear regression against volume change and time during the inter-drainage period, with the resulting rate representing the annual water supply to each lake. Our recharge rates have an uncertainty range derived by calculating a 95% confidence interval with the standard error of regression slope. These rates were compared against modelled local and total melt supplies (Table 1 in Smith et al., 2017).

2.2 *Hydraulic potential mapping and estimating subglacial water flow*

To identify likely subglacial flow routes, and therefore determine the possible location of subglacial channels, we mapped hydraulic potential (see Text S3), forced using BedMachine ice thickness and bed elevation data, assuming water pressure everywhere at overburden (Morlighem, 2019). Closed depressions within our hydropotential map were filled to represent the large-scale basal flow pattern, as discussed by Smith *et al.,* (2017). We applied a D8 routing scheme to our edited hydropotential grid to calculate the predicted motion of water throughout the glacier bed (Schwanghart & Scherler, 2014).

To gauge whether changing lake height might have an impact on the hydraulic gradients which drive water transport, background hydraulic gradients between the lakes were calculated by averaging hydraulic pressure change within each lake mask normalized by the distance between lakes. This was calculated from a hydraulic potential map without depressions filled. The background gradients represent potential gradients between each lake calculated from bed topography and ice thickness alone. During the drainage events, basal water pressure was assumed equal to ice overburden pressure and we estimated the change in potential gradients between the lakes by normalizing the change in lake height against distance along predicted flow routes. It is worth noting that as the lakes water level rises or drops, basal water pressure is likely to exceed or be less than overburden, which could introduce additional uncertainty to our change in gradients.

We allowed for the possibility that subglacial melt generated by dissipation in the subglacial network could contribute to the basal water budget. An assumption of Röthlisberger (R-)

channels was made, allowing for calculation of channel characteristics and melt production (Schoof, 2010), forced with average discharge rates (see Text S4).

2.3 *Divergence mapping*

A divergence map was derived to determine the impact of ice flow divergence on surface elevation change during the inter-drainage period. Monthly mean ice surface velocity maps of Thwaites glacier, gridded at 200m, were derived from 6 and 12 day repeat pass Sentinel-1A and -1B Synthetic Aperture Radar (SAR) data acquired in Interferometric Wide (IW) swath mode using offset tracking (Nagler *et al.,* 2015). We created a velocity composite from January 2014 to March 2017 by averaging the monthly velocity maps over the same period. Maps with less than 50% coverage of the lake region were omitted from this calculation. A divergence map was produced according to Alley *et al.* (2018), forced using our velocity composite and BedMachine ice thickness data from October 2018 (Morlighem, 2019). The length scale used to produce the maps is adaptive and based upon ice thickness multiplied by a factor of eight.

3. Results

3.1 2013 and 2017 lake drainage activities

Our timeseries of surface elevation change over the Thwaites subglacial lake system (Figure 1) captures the 2013 activity discussed by Smith *et al.,* (2017) and indicates that lake activity commenced in succession. It appears that the most upstream lake, Thw_{170}, was first to activate in early April 2013, draining until early January 2014 with a total volume loss of 0.45 ± 0.03 km^3. Second in the procession was Thw_{124}, draining from mid-May 2013 until May 2014 with a total water loss of 3.83 ± 0.11 km^3. Thw_{142} activated from early July 2013 draining until October 2013 with an average volume loss of 0.55 ± 0.03 km^3. Last in succession was Thw_{70} which drained from mid-August 2013 until May 2014 with a total water loss of 0.90 ± 0.06 km^3. Note that this succession is nearly identical to the one proposed by Smith *et al.,* (2017) except for Thw_{124}, which we find to drain later in the sequence. This disagreement is attributed to the temporal smoothing effect of the solution proposed by Smith *et al.,* (2017). We observe a second episode of lake activity upstream of Thw_{70} from early-2017, indicating a previously unobserved episode of lake drainage. Thw_{142} and Thw_{170} deflated from mid-March 2017 until mid-March 2018, with a total volume loss of 0.89 ± 0.05 km^3 and 1.91 ± 0.06 km^3 respectively, draining significantly more water than during 2013 activity. Over the same period Thw_{124} inflated by 3.20 ± 0.06 km^3 and settled 5.2 meters higher than prior to 2013 drainage. Thw_{70} shows no evidence of either drainage or recharge during 2017, remaining at a near-constant elevation.

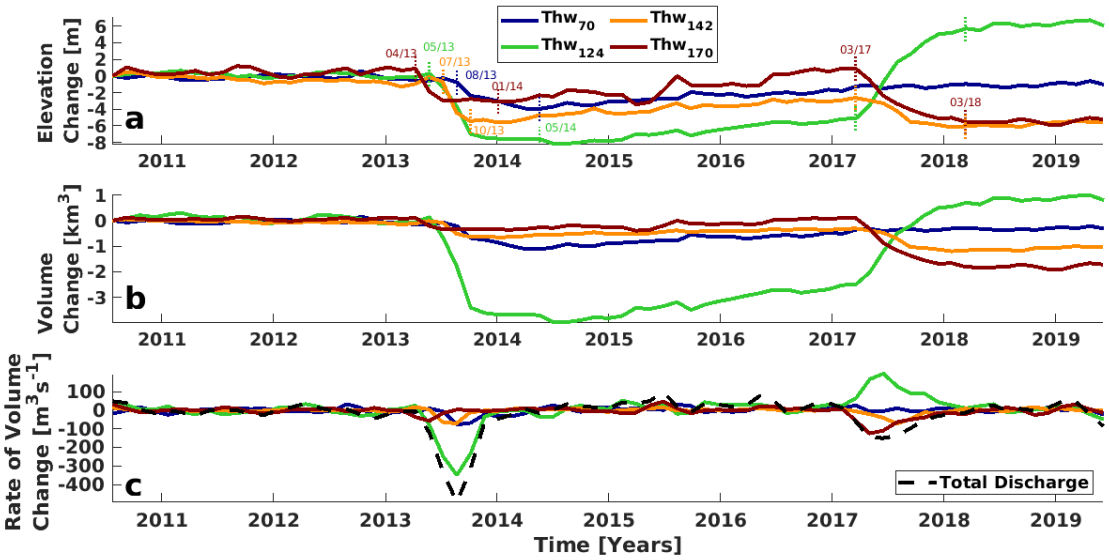

Figure 1. *Mean elevation and volume change of subglacial lakes relative to July 2010. Elevation and volume changes from 2010 until 2017 were derived assuming 2013 lake sizes, whilst 2017 to 2020 changes were derived using 2017 lake sizes. Vertical dashed lines represent the onset and termination of lake activity. (a) Mean elevation change within feature boundaries. (b) Mean volume change within feature boundaries. (c) Derivative of volume change for each lake. Black dashed line represents total discharge within the subglacial system.*

3.2 Increase in lake area

During the 2017 drainage event the upstream lakes change sized compared against the extent of activity in 2013 (Figure 2). Thw_{170} and Thw_{142} lake area expanded by 55 km^2 and 64 km^2

176 respectively, both to the east of the 2013 boundaries. Thw_{124} area decreased by 120 km^2 during
177 2017 activity, whilst maintaining the general shape of the 2013 boundary.

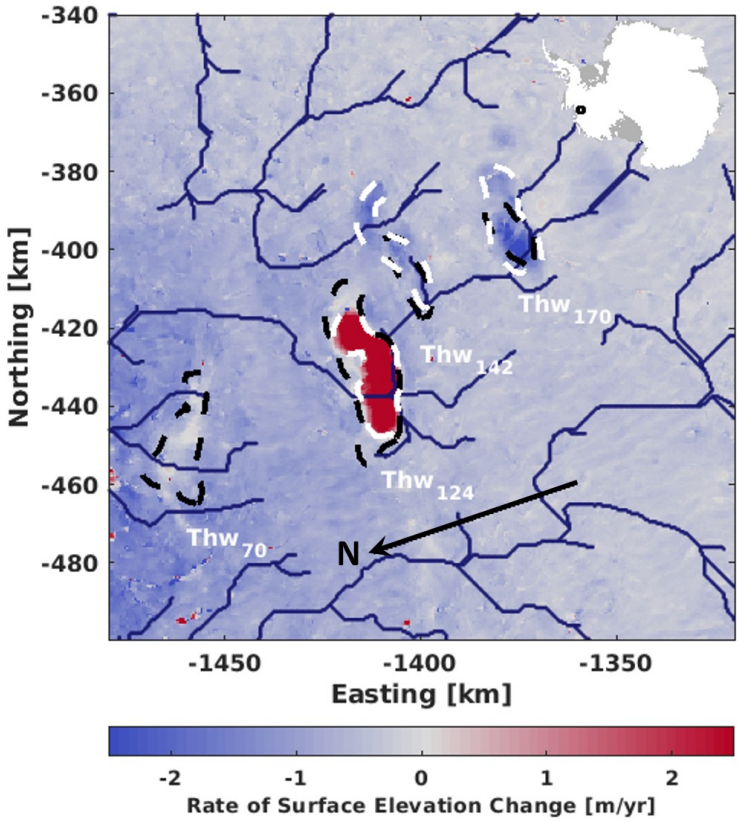

178

179 **Figure 2**. *Rates of surface elevation change for the Thwaites lake region from January 2014 to August 2019. Location of the lake*
180 *region is illustrated by the map insert. Black dashed lines represent lake boundaries during the 2013 event as described in Smith*
181 *et al., (2017). White dashed lines represent lake boundaries during the 2017 drainage event. Navy lines represent theoretical*
182 *drainage routes derived by applying a D8 routing algorithm to a hydro-potential map of the region.*

183 ### *3.3 Recharge period*

184 Following the termination of lake activity in 2014, the lakes steadily regained volume over the
185 inter-drainage period. Thw_{70}, Thw_{124}, Thw_{142}, and Thw_{170} gained 0.90 ± 0.06, 1.44 ± 0.11, 0.29 ±
186 0.03, and 0.46 ± 0.03 km^3 over 5.1, 2.6, 3.3, and 3.1 years respectively. Notably, by mid-2017,
187 Thw_{170} regained the elevation that was lost during the 2013 drainage event, whilst elevation for
188 the other lakes increased but remained below pre-2013 levels. We believe that this volume gain
189 was predominantly caused by recharge through subglacial water transport, rather than ice flow
190 divergence or blowing snow. Divergence has a negligible role, as our observations suggest an
191 impact of no more than 0.1 m yr^{-1} (see Figure S1). If blowing snow had an impact, we would
192 expect a bias in elevation change towards the prevailing wind direction – a result that we do not
193 observe (see Figures S2 and S3). These volume changes correspond to a yearly recharge rate of
194 0.18 ± 0.02, 0.57 ± 0.05, 0.10 ± 0.01 and 0.14 ± 0.03 km^3 yr^{-1} at Thw_{70}, Thw_{124}, Thw_{142}, and
195 Thw_{170} respectively. It is worth noting these rates potentially reflect the balance between positive

196 contributions from sub-glacial melt production and leakage from upstream lakes, and negative
197 contribution from leakage of the lakes into the downstream system.

198 *3.4 Water Budget*

199 Our observations of volume change for 2017 (Figure 3) can be used to determine the behavior of
200 the subglacial drainage system during the drainage activity. Both the 2013 and 2017 drainage
201 events, as well as the predicted drainage pathway (Figure 2), demonstrate the connectivity of the
202 lake system. We assume that all discharged water from the two upstream lakes directly
203 contributes to the rapid recharge of Thw_{124}. A total of 2.80 km^3 of water from the two upstream
204 lakes contributed to fill Thw_{124}, accounting for 87.5% of the observed volume gain. The
205 inclusion of Thw_{124}'s recharge rate in the budget leads to a predicted volume gain of 3.37 km^3:
206 0.17 km^3 larger than the observed increase of 3.20 km^3. This excess water falls within the
207 uncertainty range attached to our volume change estimates, which suggests that the filling at
208 Thw_{124} is a product of the drainage of the two upstream lakes and background melt production.

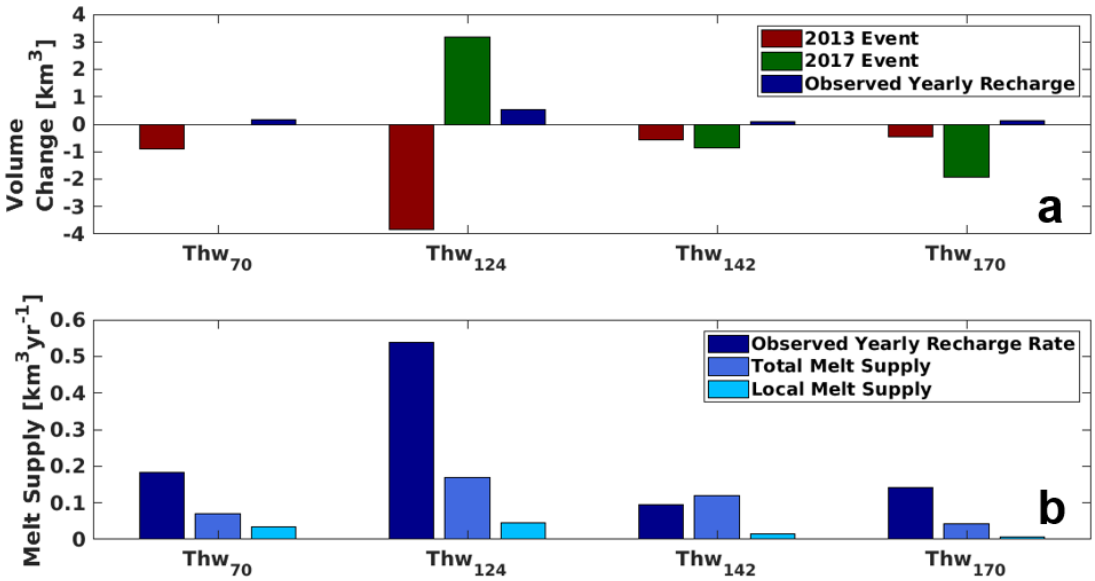

209

210 ***Figure 3.*** *Volume change and melt supply to each subglacial lake. (a) Mean volume change for the 2013 and 2017 drainage*
211 *events and estimated yearly recharge rates. Recharge rates represents average yearly volume change for each lake. (b) Different*
212 *values of potential melt supply to each feature. Local (within basin) and total (within basin and upstream) melt supply obtained*
213 *from smith et al., (2017).*

214

215 As the lakes are connected sub-glacially, any change to water levels impacts the hydraulic
216 gradients between the lakes. Background hydraulic gradients from Thw_{170} to Thw_{142}, Thw_{170} to
217 Thw_{124}, and Thw_{142} to Thw_{124} are 7.72 $x10^{-3}$, 7.64 $x10^{-3}$, and 7.83 $x10^{-3}$ respectively. During
218 2017 activity hydraulic gradients from Thw_{170} to Thw_{142}, Thw_{170} to Thw_{124} and Thw_{142} to Thw_{124}
219 decreased by 1.58 $x10^{-4}$, 5.18 $x10^{-4}$, and 1.60 $x10^{-3}$ accordingly. This represents an approximate
220 20% decrease in potential gradients against the background hydraulic gradient (see Figure S4).
221
222 *3.5 Subglacial Water Flow*

During 2013 activity Thw_{124}, Thw_{142}, and Thw_{170} displayed dynamic volume change over 240, 180, and 150 days respectively, whilst in 2017 each lake was active for approximately 300 days (Figure 1). Water fluxes also show contrasting behavior between the 2013 and 2017 events. In 2013 the rate of volume change was roughly symmetrical on either side of the peak discharge, whilst 2017 displays clear asymmetry – with post-peak discharge spanning three times the duration of pre-peak discharge.

Peak discharge reached 495.8 $m^3 s^{-1}$ in 2013, with an average discharge of 141.7 $m^3 s^{-1}$ and 84.4 $m^3 s^{-1}$ for 2013 and 2017 respectively. For individual lakes, average 2013 discharge was 34.4, 110.3, 49.3, and 16.2 $m^3 s^{-1}$ for Thw_{70}, Thw_{124}, Thw_{142}, and Thw_{170} respectively. Average 2017 discharge for Thw_{142} and Thw_{170} was 33.8 and 50.6 $m^3 s^{-1}$ respectively, considerably larger during this event than the previous. Thw_{124} gains volume at an average rate of 118.6 $m^3 s^{-1}$.

Using a simple R-channel assumption for modelling drainage pathways between the lakes, we found that average discharge rates from Thw_{170} during 2017 activity lead to a channel with cross-sectional area of 14.6 m^2 and a radius of 3.0 m. Water within this channel would flow at a mean velocity of 3.5 m s^{-1}, causing melt at the channels side walls at a rate of 0.25 $m^3 s^{-1}$. Assuming this melting rate was sustained over the period of lake activity an additional 0.008 km^3 of water would be injected into the subglacial system – negligible compared against the water mobilized from the lakes. Should channel behavior be dictated by the combined discharge from Thw_{170} and Thw_{142} we would expect a channel with a cross-sectional area of 22.1 m^2 and radius of 3.8 m. Water would flow at a mean velocity of 3.8 m s^{-1}, which corresponds to a melting rate of 0.42 $m^3 s^{-1}$. A channel of this size would contribute 0.013 km^3 of water to the subglacial system during 2017 activity.

4 Discussion

4.1 Water Budget

The net volume change of the ice sheet must be conserved from principles of mass conservation. Therefore, observing the flux of each lake allows us to infer the movement of water throughout the subglacial system. Thw_{124} appears to be the downstream limit of the drainage event in 2017. Hence, we assume that water discharged from upstream lakes combined with Thw_{124} recharge rate and drainage-related melting of the channels side was responsible for the observed volume gain. Under this assumption we expect to see a volume gain of 3.37 km^3, which is 0.17 km^3 greater than the actual volume gain observed at Thw_{124} - but falls within the uncertainty range. Background recharge rates are required to close the water budget, as without this component the water supply into Thw_{124} would be too low to explain the observed volume gain. Unlike in 2013, where the four lakes drained out of the system, there is no evidence of subglacial lake activity downstream of Thw_{124} in 2017 (Figure 1).

4.2 *Notable differences in behavior between drainage events*

Our observations highlight a marked difference in the rate and evolution of water movement between lakes during the 2013 and 2017 events. First: during the 2013 drainage event lake activity followed a cascading pattern spanning six months, whilst in 2017 all lakes activated nearly simultaneously (Figure 1). Second: volume change, average and peak discharge at Thw_{170} were significantly larger in 2017, being 324%, 212%, and 89% respectively above that of the

2013 activity. Third: Thw_{170} drained at a similar elevation in 2013 and 2017, whilst Thw_{142} drained below its 2013 level and Thw_{124} exceeded 2013 levels in 2017 without triggering drainage. Fourth: both Thw_{142} and Thw_{170} settled at a lower elevation in 2017 relative to 2013 (Figure 1a), suggesting the upstream lakes only experienced partial drainage in 2013.

Despite the apparent simultaneous activity in 2017, we suspect the lakes activity followed a cascading pattern, similar to what occurred in 2013, but with a significantly faster transfer of water that our timeseries temporal resolution could not resolve. In such a scenario, Thw_{170} would activate first and trigger Thw_{142}, with discharged water filling Thw_{124}. This scenario is further evident considering that Thw_{170} drained at similar volumes in 2013 and 2017, which suggests the lake overcame its hydro-potential barrier during both drainage events. Therefore, Thw_{170} could be considered the trigger to lake activity within the system and might be responsible for controlling future drainage events.

The rapid transfer of water in 2017 might have been made possible due to the development of a more efficient drainage system, likely following 2013 activity. Several possible mechanisms could be responsible for this change. For instance, discharge rates from the 2013 drainage event might have caused the formation of a channelized system between the lakes. While such channels would likely shrink due to creep closure, they may not have fully closed due to the transfer of water between the lakes during the inter-drainage period. This could precondition the system, allowing for rapid channel expansion during 2017 activity. Alternatively, discharge from the 2013 event might have caused sediment mobilization and potential channel erosion, leading the development of a more efficient drainage system (Brisbourne et al., 2017; Kirkham et al., 2019). Our reasoning is speculative as there is insufficient evidence available to either validate or negate these hypotheses. Nevertheless, this change in efficiency indicates complex behavior of the subglacial system, which is deserving of further study.

Discharge rates displayed a clear symmetrical ramp up and descent pattern in 2013 (Figure 1c). Conversely, discharge rates in 2017 spiked rapidly before tailing off over six months. All lakes drained in 2013 indicating an open system, whilst in 2017 the subglacial system could be considered closed, with a limit at Thw_{124} which collected water and prevented significant discharge downstream. The influx of water into Thw_{124} would have increased the pressure head within the lake, while the pressure head of upstream features was decreased due to the lower water levels. Potential gradients between the features decreased by 20%, which might have been sufficient to prolong the discharge of upstream water. Hence, the prolonged tail of discharge rates in 2017.

4.3 Observations regarding Thw_{124}

The conditions and triggers of lake drainage are still poorly understood. While Thw_{170} likely acted as a trigger for both 2013 and 2017 events, Thw_{124} displayed contrasting behavior. Thw_{124} drained in 2013 but not in 2017, despite larger upstream discharge and the fact that the lake water level, following termination of 2017 activity, exceeded that of pre-2013 drainage (Figure 1). This suggests that Thw_{124} could be acting like a roadblock, collecting water whilst preventing significant discharge downstream. The shut-down of downstream drainage could have taken place as early as mid-2014 during the onset of lake refill (Figure 1), in particular because Thw_{124} refill took place at a rate three-fold higher than at any of the other lakes (Figure 3) and that

307 modelling does not predict such a significant difference in refill rates between lakes (Smith et al.,
308 2017).

309 The mechanism behind the change in behavior of Thw_{124} is uncertain. As hypothesized earlier,
310 the significant discharge rates from 2013 activity might have modified the hydraulic properties
311 of the system, which might have formed a barrier to flow downstream. Alternatively, it could be
312 related to the mode of channel formation. Recent modelling suggests that the accumulation of
313 water within lake basins steepens the hydraulic gradient and allows greater flux downstream,
314 which melts channels that can trigger drainage (Dow et al., 2016, Dow et al., 2018). Prior to
315 2013 activity Thw_{124} appeared to be at hydrostatic equilibrium, whereby flow into the lake is
316 equal to flow out, evident by the sustained overall lake volume (Figure 1). This outwards flow
317 might have melted small channels immediately downstream of the lake. During 2013 activity,
318 when water from upstream reached Thw_{124}, hydraulic gradients would steepen. This would force
319 water over the downwards slope, melting larger channels and likely triggering drainage. As the
320 drainage event tails off, discharge rates decrease causing creep closure within the channels.
321 During the inter-drainage period, the behavior of the system changes which limits the amount of
322 water discharged from Thw_{124}, which would hamper the creation of channels. The influx of
323 water from the 2017 event would increase hydropotential gradients between the lake and
324 downstream, driving water over the reverse slope. However, inefficient downstream channels
325 might have prevented drainage.

326 *4.4 Recharge rates*

327 Our annual recharge rates are significantly above estimations based on simulations of melt
328 generation and water routing, whether considering melt production over local or regional
329 catchments (Smith et al., 2017). There is a degree of variability between lakes, with rates at
330 Thw_{70}, Thw_{124}, and Thw_{170} significantly above predicated recharge, whilst Thw_{142} is close to the
331 high-end estimate of Smith et al., (2017) (Figure 3b). The variability between predicted and
332 observed recharge rates can be explained by lake-to-lake water transfer, along with uncertainty in
333 the subglacial network. However, the overall discrepancy between our observed rates and
334 modelled values suggest estimates of melting rates at the bed are likely substantially
335 underestimated. It is likely modelled subglacial melt production was underestimated, at least in
336 part, because modelled melt did not incorporate the elevated geothermal heat flux that has been
337 suggested based on radar observations located within the Thwaites lakes' catchments (Schroeder
338 et al., 2014). In particular, Schroeder et al., (2014) suggests there may localized hot spots where
339 heat flux is greater than the background. Alternatively, the catchment and water routing used in
340 Smith et al., (2017) may not be representative of the true conditions at the bed, impacting the
341 accuracy of their derived recharge rates. Our altimetrically derived recharge rates seemingly
342 imply the second scenario of Smith et al., (2017): whereby lakes regain discharged water using
343 within catchment-scale melt production and water supplied from upstream. Assuming Thw_{70},
344 Thw_{142}, and Thw_{170} recharge at the same rate as per the inter-drainage period we expect each
345 lake to regain its pre-2013 levels in 3.2, 11.5, and 13.6 years respectively. Estimates derived
346 from modelled total melt production instead imply a recharge time of 8.1, 9.6, and 43.4 years for
347 Thw_{70}, Thw_{142} and Thw_{170} respectively. Given Thw_{170} likely triggered the 2013 and 2017

drainage events, and will likely trigger future events, the significantly shorter recharge time implies the drainage cycle of the system is shorter than previously thought.

5 Conclusions

In mid-2013 a system of interconnected subglacial lakes under the central part of the Thwaites glacier drained (Smith et al., 2017). Our altimetry measurements reveal a second period of lake activity in 2017, with discharged water tracked throughout the system. Both events are compatible with a cascading transfer of water, initiated by the most upstream lake. Observations reveal significant differences between the 2013 and 2017 drainage events. Unlike 2013 activity, in 2017 a downstream lake acts as a limit for the movement of subglacial water. This lake displayed rapid recharge, forced with discharge from the upstream lakes, increased in volume by 3.20 km^3 and settled 5.2 m higher than pre-2013 levels. Across the lake system, discharge is 29% greater in 2017 than in 2013 with lake sizes expanding by 119 km^2. During 2013 activity each lake initiated within a six-month period, whilst in 2017 the lakes activated within 45-days of each other. These characteristics point towards an increase in efficiency of the active subglacial system in 2017. Observations during the inter-drainage period indicate that lake recharge rates are 137% higher than modelled estimates. This implies that subglacial lakes recharge using melt supplied from local and upstream sources, and that geothermal heat flux and basal friction produce more melt water than currently predicted.

Acknowledgements

This work was performed at the University of Edinburgh under grants from the European Space Agency's project 4DAntarctica (ESA: Grant #4000128611/19/I-DT), and from the PROPHET project, a component of the International Thwaites Glacier Collaboration (ITGC). Support from National Science Foundation (NSF: Grant #1739031) and Natural Environment Research Council (NERC: Grants NE/S006745/1, NE/S006796/1 and NE/T001607/1). ITGC Contribution No. 024. G.R.M. acknowledges a NERC PhD Studentship. The authors wish to thank ESA for providing open access to CryoSat-2 data, and M. Morlighem for open access to Bedmachine. The authors are grateful to the editor, Mathieu Morlighem, and to two anonymous reviewers, whose comments have significantly improved the manuscript.

Data Availability Section

Our rate of change maps, lake masks and lake timeseries are freely available from 4D Antarctica (https://4d-antarctica.org/products/). The CryoSat-2 satellite altimetry data are freely available from the European Space Agency (https://earth.esa.int/web/guest/data-access). The BedMachine ice thickness and bed elevation data are freely available from the National Snow and Ice Data Centre (https://nsidc.org/data/NSIDC-0756/versions/1). The ice velocity products are based on Copernicus Sentinel-1 data made available through the European Space Agency; the products are available upon request (http://cryoportal.enveo.at). The wind velocity and direction data are freely available from the Physical Sciences Laboratory (https://psl.noaa.gov/data/gridded/data.ncep.reanalysis.derived).

References

Alley, K. E., Scambos, T. A., Anderson, R. S., Rajaram, H., Pope, A., & Haran, T. M. (2018).

Continent-wide estimates of Antarctic strain rates from Landsat 8-derived velocity grids. *Journal of Glaciology*, *64*(244), 321–332. https://doi.org/10.1017/jog.2018.23

Alley, R. B., Blankenship, D. D., Bentley, C. R., & Rooney, S. T. (1986). Deformation of till beneath ice stream B, West Antarctica. *Nature*, *322*(6074), 57–59. https://doi.org/10.1038/322057a0

Bartholomaus, T. C., Anderson, R. S., & Anderson, S. P. (2008). Response of glacier basal motion to transient water storage. *Nature Geoscience*, *1*(1), 33–37. https://doi.org/10.1038/ngeo.2007.52

Bell, R. E. (2008, May). The role of subglacial water in ice-sheet mass balance. *Nature Geoscience*. Nature Publishing Group. https://doi.org/10.1038/ngeo186

Smith, B., Fricker, H., Joughin, I., & Tulaczyk, S. (2009). An inventory of active subglacial lakes in Antarctica detected by ICESat (2003-2008. *Journal of Glaciology*, *55*(192), 573–595. https://doi.org/10.3189/002214309789470879

Björnsson, H. (1992). Jokulhlaups in Iceland: prediction, characteristics and simulation. *Annals of Glaciology*, *16*, 95–106. https://doi.org/10.3189/1992aog16-1-95-106

Björnsson, H. (2002). Subglacial lakes and jökulhlaups in Iceland. *Global and Planetary Change*, *35*(3), 255–271. https://doi.org/10.1016/S0921-8181(02)00130-3

Brisbourne, A. M., Smith, A. M., Vaughan, D. G., King, E. C., Davies, D., Bingham, R. G., et al. (2017). Bed conditions of Pine Island Glacier, West Antarctica. *Journal of Geophysical Research: Earth Surface*, *122*(1), 419–433. https://doi.org/10.1002/2016JF004033

Le Brocq, A. M., Ross, N., Griggs, J. A., Bingham, R. G., Corr, H. F. J., Ferraccioli, F., et al. (2013). Evidence from ice shelves for channelized meltwater flow beneath the Antarctic Ice Sheet. *Nature Geoscience*, *6*(11), 945–948. https://doi.org/10.1038/ngeo1977

Dow, C. F., Werder, M. A., Nowicki, S., & Walker, R. T. (2016). Modeling Antarctic subglacial lake filling and drainage cycles. *The Cryosphere*, *10*(4), 1381–1393. https://doi.org/10.5194/tc-10-1381-2016

Dow, C. F., Werder, M. A., Babonis, G., Nowicki, S., Walker, R. T., Csatho, B., & Morlighem, M. (2018). Dynamics of Active Subglacial Lakes in Recovery Ice Stream. *Journal of Geophysical Research: Earth Surface*, *123*(4), 837–850. https://doi.org/10.1002/2017JF004409

Flament, T., Berthier, E., & Rémy, F. (2014). Cascading water underneath Wilkes Land, East Antarctic ice sheet, observed using altimetry and digital elevation models. *The Cryosphere*, *8*(2), 673–687. https://doi.org/10.5194/tc-8-673-2014

Foresta, L., Gourmelen, N., Pálsson, F., Nienow, P., Björnsson, H., & Shepherd, A. (2016).

Surface elevation change and mass balance of Icelandic ice caps derived from swath mode CryoSat-2 altimetry. *Geophysical Research Letters*. https://doi.org/10.1002/2016GL071485

Fowler, A. C. (1999). Breaking the seal at Grímsvötn, Iceland. *Journal of Glaciology*, *45*(151), 506–516. https://doi.org/https://doi.org/10.3189/S0022143000001362

Fretwell, P., Pritchard, H. D., Vaughan, D. G., Bamber, J. L., Barrand, N. E., Bell, R., et al. (2012). Bedmap2: improved ice bed, surface and thickness datasets for Antarctica The Cryosphere Discussions Bedmap2: improved ice bed, surface and thickness datasets for Antarctica. *TCD*, *6*(6), 4305–4361. https://doi.org/10.5194/tcd-6-4305-2012

Fricker, H. A., Carter, S. P., Bell, R. E., & Scambos, T. (2014). Active lakes of recovery ice stream, East Antarctica: A bedrock-controlled subglacial hydrological system. *Journal of Glaciology*, *60*(223), 1015–1030. https://doi.org/10.3189/2014JoG14J063

Fricker, H. A., & Scambos, T. (2009). Connected subglacial lake activity on lower Mercer and Whillans Ice Streams, West Antarctica, 2003-2008. *Journal of Glaciology*, *55*(190), 303–315. https://doi.org/10.3189/002214309788608813

Fricker, H. A., Scambos, T., Bindschadler, R., & Padman, L. (2007). An active subglacial water system in West Antarctica mapped from space. *Science*, *315*(5818), 1544–1548. https://doi.org/10.1126/science.1136897

Gourmelen, N., Escorihuela, M. J., Shepherd, A., Foresta, L., Muir, A., Garcia-Mondéjar, A., et al. (2018). CryoSat-2 swath interferometric altimetry for mapping ice elevation and elevation change. *Advances in Space Research*, *62*(6), 1226–1242. https://doi.org/10.1016/j.asr.2017.11.014

Gray, L., Burgess, D., Copland, L., Cullen, R., Galin, N., Hawley, R., & Helm, V. (2013). Interferometric swath processing of Cryosat data for glacial ice topography. *Cryosphere*, *7*(6), 1857–1867. https://doi.org/10.5194/tc-7-1857-2013

Gray, L., Burgess, D., Copland, L., Demuth, M. N., Dunse, T., Langley, K., & Schuler, T. V. (2015). CryoSat-2 delivers monthly and inter-annual surface elevation change for Arctic ice caps. *Cryosphere*, *9*(5), 1895–1913. https://doi.org/10.5194/tc-9-1895-2015

Gray, Laurence. (2005). Evidence for subglacial water transport in the West Antarctic Ice Sheet through three-dimensional satellite radar interferometry. *Geophysical Research Letters*, *32*(3), L03501. https://doi.org/10.1029/2004GL021387

Gray, Laurence, Burgess, D., Copland, L., Langley, K., Gogineni, P., Paden, J., et al. (2019). Measuring Height Change Around the Periphery of the Greenland Ice Sheet With Radar Altimetry. *Frontiers in Earth Science*, *7*. https://doi.org/10.3389/feart.2019.00146

Hawley, R. L., Shepherd, A., Cullen, R., Helm, V., & Wingham, D. J. (2009). Ice-sheet

elevations from across-track processing of airborne interferometric radar altimetry. *Geophysical Research Letters*, *36*(22). https://doi.org/10.1029/2009GL040416

Joughin, I., Tulaczyk, S., Bamber, J. L., Blankenship, D., Holt, J. W., Scambos, T., & Vaughan, D. G. (2009). Basal conditions for Pine Island and Thwaites Glaciers, West Antarctica, determined using satellite and airborne data. *Journal of Glaciology*, *55*(190), 245–257. https://doi.org/10.3189/002214309788608705

Kalnay, E.; Kanamitsu, M.; Kistler, R.; Collins, W.; Deaven, D.; Gandin, L.; Iredell, M.; Saha, S.; White, G.; Woollen, J. Zhu, Y.; Chelliah, M.; Ebisuzaki, W.; Higgins, W.; Janowiak, J.; MoK.C., C. Ropelewski, Wang, J.; Leetmaa, A.; Reynolds, R.; Jenne, R. and J. D. (1996). Kalnay_1996_Ncep_Reanalysis.Pdf. *Bulletin of the American Meteorological Society*, 437–471. https://doi.org/10.1175/1520-0477(1996)077<0437:TNYRP>2.0.CO;2

Kamb, B. (2001). The West Antarctic Ice Sheet: Behavior and Environment Research Series, Volume 77 (pp. 157–199). https://doi.org/10.1029/ar077p0157

Kirkham, J. D., Hogan, K. A., Larter, R. D., Arnold, N. S., Nitsche, F. O., Golledge, N. R., & Dowdeswell, J. A. (2019). Past water flow beneath Pine Island and Thwaites glaciers, West Antarctica. *The Cryosphere*, *13*, 1959–1981. https://doi.org/10.5194/tc-13-1959-2019

McMillan, M., Shepherd, A., Sundal, A., Briggs, K., Muir, A., Ridout, A., et al. (2014). Increased ice losses from Antarctica detected by CryoSat-2. *Geophysical Research Letters*. https://doi.org/10.1002/2014GL060111

Morlighem, M., Rignot, E., Binder, T., Blankenship, D., Drews, R., Eagles, G., et al. (2020). Deep glacial troughs and stabilizing ridges unveiled beneath the margins of the Antarctic ice sheet. *Nature Geoscience*, *13*(2), 132–137. https://doi.org/10.1038/s41561-019-0510-8

Nagler, T., Rott, H., Hetzenecker, M., Wuite, J., Potin, P. (2015). The Sentinel-1 Mission: New Opportunities for Ice Sheet Observations. *Remote Sensing, 7*, 9371-9389. https://doi.org/10.3390/rs70709371

Parizek, B. R., Alley, R. B., Anandakrishnan, S., & Conway, H. (2002). Sub-catchment melt and long-term stability of ice stream D, West Antarctica. *Geophysical Research Letters*, *29*(8), 55-1-55–4. https://doi.org/10.1029/2001gl014326

Rignot, E., Mouginot, J., & Scheuchl, B. (2011). Ice flow of the antarctic ice sheet. *Science*, *333*(6048), 1427–1430. https://doi.org/10.1126/science.1208336

Schoof, C. (2010). Ice-sheet acceleration driven by melt supply variability. *Nature*, *468*(7325), 803–806. https://doi.org/10.1038/nature09618

Schroeder, D. M., Blankenship, D. D., Young, D. A., & Quartini, E. (2014). Evidence for elevated and spatially variable geothermal flux beneath the West Antarctic Ice Sheet.

Proceedings of the National Academy of Sciences of the United States of America, *111*(25), 9070–9072. https://doi.org/10.1073/pnas.1405184111

Schwanghart, W., & Scherler, D. (2014). Short Communication: TopoToolbox 2-MATLAB-based software for topographic analysis and modeling in Earth surface sciences. *Earth Surf. Dynam*, *2*, 1–7. https://doi.org/10.5194/esurf-2-1-2014

Sergienko, O. V., MacAyeal, D. R., & Bindschadler, R. A. (2007). Causes of sudden, short-term changes in ice-stream surface elevation. *Geophysical Research Letters*, *34*(22), L22503. https://doi.org/10.1029/2007GL031775

Siegert, M. J., Carter, S., Tabacco, I., Popov, S., & Blankenship, D. D. (2005, September). A revised inventory of Antarctic subglacial lakes. *Antarctic Science*. https://doi.org/10.1017/S0954102005002889

Siegfried, M. R., & Fricker, H. A. (2018). Thirteen years of subglacial lake activity in Antarctica from multi-mission satellite altimetry. *Annals of Glaciology*, *59*(76pt1), 42–55. https://doi.org/10.1017/aog.2017.36

Smith, B. E., Gourmelen, N., Huth, A., & Joughin, I. (2017). Connected subglacial lake drainage beneath Thwaites Glacier, West Antarctica. *Cryosphere*, *11*(1), 451–467. https://doi.org/10.5194/tc-11-451-2017

Stearns, L. A., Smith, B. E., & Hamilton, G. S. (2008, December 16). Increased flow speed on a large east antarctic outlet glacier caused by subglacial floods. *Nature Geoscience*. Nature Publishing Group. https://doi.org/10.1038/ngeo356

Wei, W., Blankenship, D. D., Greenbaum, J. S., Gourmelen, N., Dow, C. F., Richter, T. G., et al. (2020). Getz Ice Shelf melt enhanced by freshwater discharge from beneath the West Antarctic Ice Sheet. *The Cryosphere*, *14*(4), 1399–1408. https://doi.org/10.5194/tc-14-1399-2020

Wingham, D. J., Siegert, M. J., Shepherd, A., & Muir, A. S. (2006). Rapid discharge connects Antarctic subglacial lakes. *Nature*, *440*(7087), 1033–1036. https://doi.org/10.1038/nature04660

Wright, A., & Siegert, M. (2012). A fourth inventory of Antarctic subglacial lakes. *Antarctic Science*, *24*(6), 659–664. https://doi.org/10.1017/S095410201200048X